ATMOSPHERE'S OPTICAL MICRO PARAMETERS INFLUENCE UPON POLAR-PHASE CURVES OF SCATTERED RADIATION

S.V. Korkin *

Moscow Power-Engineering Institute (TU), Light Engineering Department,
111250, Krasnokazarmennaya 14, Moscow, Russia – sergei_korkin@mail.ru

KEY WORDS: Polar-Phase Curves, Vectorial Modification of Spherical Harmonics Method, VRTE solution

ABSTRACT:

Here we describe an efficient mathematical model of polarized radiation transfer for the purposes of passive polarimeters operation. The model is built upon a new approach to the solution of a vectorial radiation transfer equation (VRTE) boundary problem based on the subtraction of VRTE solution's spatial singularities by means of the vectorial small angle modification of spherical harmonics method (VMSH) with the subsequent determination of the solution's smooth part. The atmosphere is considered as a slab of an arbitrary thickness. The angle of irradiance is arbitrary and a diffusely reflecting bottom boundary with variable reflectance was admitted. We explore the influence of the turbid media upon the spatial distribution of the polarization state of reflected or transmitted radiation by both changing of scalar parameters (single scattering albedo, optical thickness of a slab, average scattering cosine or the maximum degree of polarization state and elasticity within single scattering act for Heneye-Greenstein (HG) scattering model) and the substitution of different scattering matrix models: HG, Rayleigh, Mie.

1. INTRODUCTION

The polarization state of scattered radiation is the only and the most complete information source about a microstructure of a scattering turbid media (atmosphere, natural waters or even solid bodies if particles spin-depended scattering is considered) available for optical methods. The modern level of development of electro-optical systems (EOS) design allows constructing different types of polarimeters with a high degree of polarization state's measurement accuracy. But for the purposes of effective construction of such systems a reliable mathematical model of polarized radiation transfer (RT) is necessary. Such model together with the system construction parameters allow to obtain the signal-to-noise ratio in order to get the adequate system accuracy for observing the required polarization effects.

We consider the RT boundary problem (BP) for the vectorial radiative transfer equation (VRTE) in a slab written in usual form

$$\begin{cases} \mu \dfrac{\partial \vec{L}(\tau,\hat{\mathbf{l}})}{\partial \tau} + \vec{L}(\tau,\hat{\mathbf{l}}) = \dfrac{\Lambda}{4\pi}\int_{\Omega} \vec{R}(\chi_2')\,\bar{x}(\hat{\mathbf{l}}\hat{\mathbf{l}}')\,\vec{R}(\chi_1')\vec{L}(\tau,\hat{\mathbf{l}}')\,d\hat{\mathbf{l}}', \\ \vec{L}(0,\mu>0,\varphi) = \vec{L}_0\,\delta(\hat{\mathbf{l}}-\hat{\mathbf{l}}_0); \quad \vec{L}(\tau_0,\mu\le 0,\varphi) = \rho\vec{E}/\pi. \end{cases} \tag{1}$$

The following notation is used here and further on: $\vec{L}$ - Stokes vector (SV) depended on the optical thickness τ and an arbitrary unit direction $\hat{\mathbf{l}} = \left\{\sqrt{1-\mu^2}\cos\varphi;\ \sqrt{1-\mu^2}\sin\varphi;\ \mu\right\}$ where $\mu = a\cos\theta$; θ, φ - zenith and azimuth angles respectively, $\hat{\mathbf{l}}_0$ - the direction of irradiance of the slab by an infinitely wide unidirectional beam with initial SV set of parameters given by $\vec{L}_0 = \begin{bmatrix} 1 & p\cos(\varphi-\varphi_0) & p\sin(\varphi-\varphi_0) & q \end{bmatrix}^T$, p, q, φ_0– the linear polarization degree, the ellipticity and the reference plane position of the incident radiation respectively, δ - Dirac's delta-function that describes the point unidirectional source of light. We mark all vector columns by "→" and matrices are marked by "↔". The total optical depth of the slab is τ_0 (it is assumed to be arbitrary) and the single scattering albedo is Λ. $\vec{R}(\chi_2')$, $\vec{R}(\chi_1')$ are angle-depended rotation matrices (rotators) that serve to rotate the frame of reference within scattering act described by scattering matrix $\bar{x}(\hat{\mathbf{l}}\hat{\mathbf{l}}')$. We assumed the bottom boundary to be a Lambertian one with the reflectance ρ and the irradiance vector $\vec{E}$.

The described delta-function, singularity in other words, prevents one from the direct calculation of radiation field for this singularity has the infinity spatial spectrum. That is why only scattered radiation can be computed but only after the procedure of singularity subtraction – the well known standard approach (Chandrasekhar, 1960). The obtained difference field can be computed by finite expansion series but for the case of real scattering media with a high degree of scattering anisotropy the expansion series may occur too long. This fact will cause numerous calculations and may even result in the ill-conditionality of the VRTE BP solution. Further on we give the approach that will help to eliminate the described problem (Budak, 2004).

2. METHOD OF SOLUTION

2.1 The anisotropic part determination

The singularity we are having a deal with and physically natural ray approximation widely used in optics of turbid media cause the smoothness of spatial spectrum of the desired vectorial light

* Corresponding author.

field $\vec{L}(\tau,\hat{\mathbf{l}})$ given in the known circular basis (CP) (Kuščer, 1959) as the series

$$\vec{L}_{\mathrm{CP}}(\tau,\hat{\mathbf{l}}) = \sum_{m=-\infty}^{\infty}\sum_{k=0}^{\infty}\frac{2k+1}{4\pi}\vec{Y}_m^k(\mu)\vec{f}_m^k(\tau)\exp(im\varphi), \qquad (2)$$

$$\vec{Y}_m^k(\mu) = \mathrm{Diag}\left[\mathrm{P}_{m,+2}^k(\mu);\ \mathrm{P}_{m,+0}^k(\mu);\ \mathrm{P}_{m,-0}^k(\mu);\ \mathrm{P}_{m,-2}^k(\mu)\right]$$

and $\mathrm{P}_{m,n}^k(\mu)$ is the generalized spherical function (harmonic – GSH) depended on the zenith index (the order) k, the index of azimuth expansion m and polarization index n. The singularity together with the significant scattering anisotropy degree of phase functions of real media which can also be represented on the GSH expansion as (r, s = 2, 0, – 0, – 2)

$$\left[\vec{x}(\hat{\mathbf{H}})\right]_{r,s} = \sum_{k=0}^{\infty}(2k+1)x_{r,s}^k(\tau)\mathrm{P}_{r,s}^k(\hat{\mathbf{H}}),$$

allow one to restrict the number of SV GSH expansion terms in Taylor series to two terms. The expansion of the spatial spectrum is obtained with respect to GSH order k provided this order to be a continuous one. This gives comparatively simple expression for spatial spectrum amplitudes (i.e. the GSH expansion coefficients) as exponential matrix. This form of approximate solution is called the vectorial small-angle modification of spherical harmonics method (VMSH) (Astakhov, 1994). It has an analytical form, describes all VRTE solution's singularities, gives the most anisotropic part of light field quite accurately (almost the whole forward hemisphere for many real cases (Budak, 2008)) and can be computed fast using simple PC (some seconds). The VMSH has the following form in the Stokes polarization (SP) basis after the eliminating of complex components

$$\vec{L}_{\mathrm{VMSH}}(\tau,\hat{\mathbf{H}}_0) = \sum_{k=0}^{\infty}\frac{2k+1}{4\pi}\left\{\vec{P}_R^{k,0}(\nu)\vec{Z}_k(\tau)\begin{bmatrix}2\\0\\0\\2q\end{bmatrix} - \right.$$

$$\left. -\vec{P}_R^{k,2}(\nu)\vec{Z}_k(\tau)\begin{bmatrix}0\\p\cos 2\Delta\varphi\\p\sin 2\Delta\varphi\\0\end{bmatrix} - \vec{P}_I^{k,2}(\nu)\vec{Z}_k(\tau)\begin{bmatrix}0\\-p\sin 2\Delta\varphi\\p\cos 2\Delta\varphi\\0\end{bmatrix}\right\}, \qquad (3)$$

We use the following notation in (3)

$$\vec{P}_R^{k,m}(\nu) = \mathrm{diag}\left[\mathrm{Q}_m^k(\nu);\mathrm{R}_m^k(\nu);\mathrm{R}_m^k(\nu);\mathrm{Q}_m^k(\nu)\right];$$

$$\mathrm{R}_m^k(\mu) = \frac{1}{2}\left[\mathrm{P}_{m,2}^k(\mu)+\mathrm{P}_{m,-2}^k(\mu)\right];\ \mathrm{T}_m^k(\mu) = \frac{1}{2}\left[\mathrm{P}_{m,2}^k(\mu)-\mathrm{P}_{m,-2}^k(\mu)\right];$$

$$\vec{P}_I^{k,m}(\nu) = \begin{bmatrix}0&0&0&0\\0&0&-\mathrm{T}_m^k(\nu)&0\\0&\mathrm{T}_m^k(\nu)&0&0\\0&0&0&0\end{bmatrix};\ \vec{Z}_k = \exp\left[-\frac{(\vec{1}-\Lambda\vec{\chi}_k)\tau}{\mu_0}\right];$$

$$\Delta\varphi = \psi + \varphi_0.$$

and $\mathrm{Q}_m^k(\nu)$ are Schmidt semi-normalized polynomials.

We note here that (3) is written in the incident ray frame of reference: the "zenith" angle with its cosine $\nu = \hat{\mathbf{H}}\hat{\mathbf{H}}_0$ is counted off from the direction of irradiance $\hat{\mathbf{l}}_0$ and azimuth angle ψ is counted off in the plane being perpendicular to $\hat{\mathbf{l}}_0$. So the equations $\mu = \nu$ and $\varphi = \psi$ are true only for normal irradiance of the slab. The scattering matrix spatial spectrum is $\vec{\chi}_k$.

We give an example of VMSH calculation itself. Here and further on we use the polarization degree defined with respect to parallel (l) and perpendicular (r) components as

$$p(\theta) = \frac{\mathrm{L}_l(\theta)-\mathrm{L}_r(\theta)}{\mathrm{L}_l(\theta)+\mathrm{L}_r(\theta)} = \frac{\mathrm{Q}(\theta)}{\mathrm{I}(\theta)}. \qquad (4)$$

Heneye-Greenstein (HG) scattering matrix was used with maximum linear polarization degree within single scattering act P_m = 0.5 and the same for ellipticity Q_m = 0.5, Λ = 0.9, τ = 5. Different average scattering cosine g = 0.97 and 0.7 was used. The result obtained by VMSH is compared with standard discrete ordinates method (DOM). The angle of irradiance θ_o = 30°.

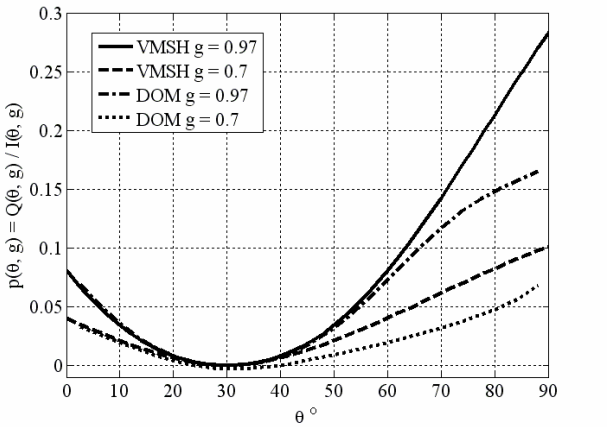

Figure 1. Polarization degree with respect to different average scattering cosine *g*. VMSH and DOM results.

One can see from Figure 1 that the greater is the scattering anisotropy – the larger is the area of VMSH validity. This are of validity is always called "the small angle area". But these small angles spread within the area approximately ± tens of degrees ($\pm 30^o$ for considered case of oceanic scattering g = 0.97 that needs 350 harmonics for VMSH and less than 7 seconds of computation time) and within the desirable accuracy – and so the VMSH itself can serve for analyse the descending (from the Sun to the Earth) radiation's polarization properties.

But for the case of wide-angles scattering and ascending from the Earth radiation (diffusely reflected from the slab) a discrepancy between the VMSH and the exact solution must be obtained. The VMSH being the source function for VRTE's boundary problem (with boundary conditions modified accordingly to the new source function) allows to obtain a

smooth (regular or non-small angle) part which enlarge the VMSH to the complete VRTE analytical solution. The smoothness of the regular part allows not to produce numerous calculations. This fact together with fast computing of the VMSH and the known scale transformation operation (Karp, 1980) determines the computation efficiency and the solution's stability of the described method. Boundary conditions in the form of Mark allows to consider an arbitrary reflecting properties of the bottom of a scattered media especially if matrix discrete ordinates method is used. The important advantage of the VMSH as a source function concludes in the fact that the VRTE boundary problem does not change its form and the smooth part can be efficiently evaluated by means of well known and deeply investigated methods such as discrete ordinates (DOM) or spherical harmonics methods (SHM), Monte-Carlo simulation an so on. The regular part will be found in the next part of the paper.

2.2 The regular part's boundary problem

Let's represent the complete solution of (1) as the superposition of the VMSH (marked with index S – singular part) and discrepancy (marked with index R – regular part)

$$\vec{L}(\tau,\hat{\mathbf{l}}) = \vec{L}_S(\tau,\hat{\mathbf{l}}) + \vec{L}_R(\tau,\hat{\mathbf{l}}) \qquad (5)$$

This will convert BP (1) to

$$\begin{cases} \mu\dfrac{\partial\vec{L}_R(\tau,\hat{\mathbf{l}})}{\partial\tau} + \vec{L}_R(\tau,\hat{\mathbf{l}}) = \dfrac{\Lambda}{4\pi}\int\vec{X}(\hat{\mathbf{l}},\hat{\mathbf{l}}',\chi_2',\chi_1')\vec{L}_R(\tau,\mathbf{l}')\,d\hat{\mathbf{l}}' + \\ + \vec{\Delta}(\tau,\hat{\mathbf{l}}); \qquad \vec{L}_R(0,\mu>0,\varphi) = \vec{0}; \\ \vec{L}_R(\tau_0,\mu\le 0,\varphi) = \rho\vec{E}/\pi - \vec{L}_S(\tau_0,\mu\le 0,\varphi) \end{cases} \qquad (6)$$

$$\vec{X}(\hat{\mathbf{l}},\chi_2',\chi_1') = \vec{R}(\chi_2')\vec{x}(\hat{\mathbf{l}})\vec{R}(\chi_1')$$

The source function has the form based on the VMSH

$$\vec{\Delta}(\tau,\hat{\mathbf{l}}_0) = (\mu_0-\mu)\frac{\partial}{\partial\tau}\vec{L}_S(\tau,\hat{\mathbf{l}}_0) \qquad (7)$$

We'll seek for solution of (6) similar to the solution of (1) represented as the following (Siewert, 2000)

$$\vec{L}(\tau,\hat{\mathbf{l}}) = \sum_{m=0}^{\infty}(2-\delta_{0,m})\left[\phi_1(m\varphi)\vec{L}_1(\tau,\mu) + \phi_2(m\varphi)\vec{L}_2(\tau,\mu)\right], \qquad (8)$$

$$\phi_1(\varphi) = \mathrm{diag}\left[\cos\varphi,\ \cos\varphi,\ \sin\varphi,\ \sin\varphi\right]$$

$$\phi_2(\varphi) = \mathrm{diag}\left[-\sin\varphi,\ -\sin\varphi,\ \cos\varphi,\ \cos\varphi\right].$$

In order to do this we must transform VMSH (3) from the {ν, ψ} frame of reference to {μ, φ} one using the rotator. We have after this ($\delta_{0,m}$ is the Kronecker symbol)

$$\vec{L}_S(\tau,\hat{\mathbf{l}}) = \sum_{c=1,2}\sum_{k=0}^{\infty}\frac{2k+1}{4\pi}\sum_{m=0}^{k}(2-\delta_{0,m})\vec{\phi}_c(m\varphi)\vec{A}_m^k(\mu,\mu_0,\tau)\vec{D}_c\vec{L}_0, \qquad (9)$$

where $\vec{A}_m^k(\mu,\mu_0,\tau) = \vec{\Pi}_m^k(\mu)\vec{Z}_k(\tau)\vec{\Pi}_m^k(\mu_0)$ and

$$\vec{\Pi}_m^k(\mu) = \begin{bmatrix} Q_k^m(\mu) & 0 & 0 & 0 \\ 0 & R_k^m(\mu) & -T_k^m(\mu) & 0 \\ 0 & -T_k^m(\mu) & R_k^m(\mu) & 0 \\ 0 & 0 & 0 & Q_k^m(\mu) \end{bmatrix}.$$

Having substituted (9) into (7) and using the recurrence formula for new basic matrix Π-polynomials

$$\mu\vec{\Pi}_m^k(\mu) = \frac{1}{2k+1}\left[\vec{A}_{k+1}^m\vec{\Pi}_m^{k+1}(\mu) + \vec{B}_k^m\vec{\Pi}_k^m(\mu) + \vec{A}_k^m\vec{\Pi}_m^{k-1}(\mu)\right],$$

$$\left[\vec{A}_m^k\right]_{rs} = \frac{1}{k}\sqrt{\left(k^2-m^2\right)\left(k^2-s^2\right)}\delta_{rs};\ \left[\vec{B}_m^k\right]_{rs} = -\frac{2m}{k\left(k+1\right)}\left(2k+1\right)\delta_{r,-s};$$

$$r,s = +0,+2,-2,-0$$

which one can easily prove using the recurrence formulas for ordinary GSH (Gelfand, 1963) and after the eliminating of complex terms (see (2)) we obtain the following expression for the source function in energetic SP basis

$$\vec{\Delta}(\tau,\hat{\mathbf{l}}_0) = \frac{1}{4\pi}\sum_{c=1,2}\sum_{k=0}^{\infty}\sum_{m=0}^{k}(2-\delta_{0,m})\times$$

$$\times\left[\frac{1}{\mu_0}\vec{\phi}_c(m\varphi)\left\{\vec{A}_{k+1}^m\vec{\Pi}_m^{k+1}(\mu) + \vec{B}_k^m\vec{\Pi}_m^k(\mu) + \vec{A}_k^m\vec{\Pi}_m^{k-1}(\mu)\right\}\times\right. \qquad (10)$$

$$\times(\vec{1}-\Lambda\vec{\chi}_k)\exp\left[-\frac{(\vec{1}-\Lambda\vec{\chi}_k)\tau}{\mu_0}\right]\vec{\Pi}_m^k(\mu_0)\vec{D}_c -$$

$$\left.\vec{\phi}_c(m\varphi)(2k+1)\vec{\Pi}_m^k(\mu)(\vec{1}-\Lambda\vec{\chi}_k)\exp\left[-\frac{(\vec{1}-\Lambda\vec{\chi}_k)\tau}{\mu_0}\right]\vec{\Pi}_m^k(\mu_0)\vec{D}_c\right]\vec{L}_0$$

And finally after evaluating the scattering integral the BP for regular part can be solved using any of the known methods – discrete ordinates method (DOM), spherical harmonics method, Monte-Carlo simulation and so on. DOM together with the boundary conditions written in the form of Mark allows to consider an arbitrary spatial distribution of the reflecting properties of the bottom bound easily. For the case of DOM the VRTE is reduced to the set of differential equations – independent for each m^{th} azimuth harmonic and for each of the two terms of (8)

$$\mu_i\frac{\partial}{\partial\tau}\vec{L}_c^m(\tau,\mu_i) = -\vec{L}_c^m(\tau,\mu_i) +$$

$$+\frac{\Lambda}{2}\sum_{k=0}^{K}\sum_{j=1}^{N}(2k+1)w_j\vec{\Pi}_m^k(\mu_i)\vec{\chi}_k\vec{\Pi}_m^k(\mu_j)\vec{L}_c^m(\tau,\mu_j) + \vec{\Delta}_c^m(\tau,\mu_i). \qquad (11)$$

The VMSH in the form of (9) allows to obtain the boundary conditions for each m and to obtain the source function in the appropriate frame of reference. But we note that the anisotropic part itself must be computed using(3). And only to (3) one should add the solution of (11).

2.3 The computation features of the method

We made the comparison o the proposed approach with other method in (Budak, 2008b) and so for the sake of shortness we will not repeat that results here. Now we only give some computations to show some features of the described approach.

We consider a slab with HG scattering (P_m = 0.5, Q_m = 0 (Hovenier, 1996)) and average scattering cosine g = 0.9, Λ = 0.8, τ = 1. The bottom boundary is considered non reflective with ρ = 0. Angle of irradiance is $\theta_o = 40^o$, incident light is natural (nonpolarized). We use M_{DOM} = 28 azimuthal harmonics to compute the Q-component of the SV spatial distribution within forward hemisphere – transmitted radiation. This amount of harmonics is enough for the solution does not vary for larger amount of them. The solution obtained with standard method (Chandrasekhar, 1960) is marked with circles on Figure 2. For our approach we need only $M_{VMSH+DOM}$ = 10 azimuthal harmonics in order to obtain the same result – solid line on the Figure 2

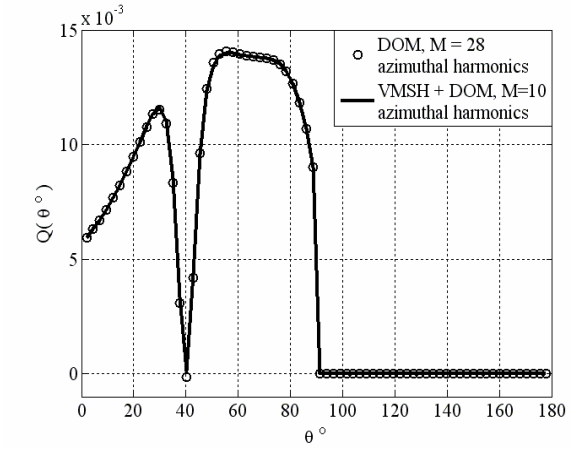

Figure 2. Q-component zenith distribution for different azimuthal expansion orders of VMSH + DOM and DOM.

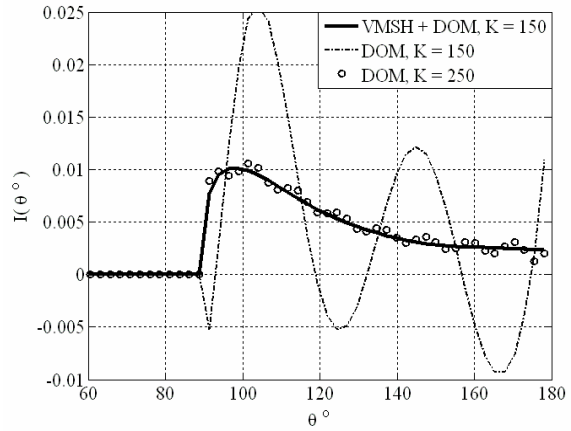

Figure 3. I-component zenith distribution for different zenith expansion orders of VMSH + DOM and DOM.

Let's consider the same slab with HG scattering but for average scattering cosine g = 0.97, Λ = 0.9, τ = 5. The bottom boundary is considered non reflective again, the irradiance with natural light is normal. We use K_{DOM} = 250 zenith harmonics to compute the I-component of the SV spatial distribution within backward hemisphere – the reflected radiation. Again the solution obtained with standard method is marked with circles on Figure 3 and some oscillation is still evident. For our approach we need only $K_{VMSH+DOM}$ = 150 azimuthal harmonics in order to obtain the same result – solid line on the Figure 3. The amount of 150 harmonics for standard method gives hard oscillations. We note here that this advantage in zenith expansion preserves for every of azimuth harmonics for the system of differential equations for them are independent but the zenith GSH expansion of the desired solution and the phase function (phase matrix in general case) are the same for each azimuth term.

3. THE INFLUENCE OF THE BOTTOM REFLECTION

First of all we give some results for diffusely and hence completely depolarized bottom boundary with the reflectance coefficient noted as ρ and Mueller matrix given by diagonal matrix of the form $\vec{M}(\vec{\mu},\vec{\mu}') = \mathrm{diag}[\rho;0;0;0]$. The influence of the reflecting boundary can be easily investigated by applying boundary problem decomposition method to (1). Water Haze L approximation (Deirmendjian, 1969) was used as the Mie scattering model.

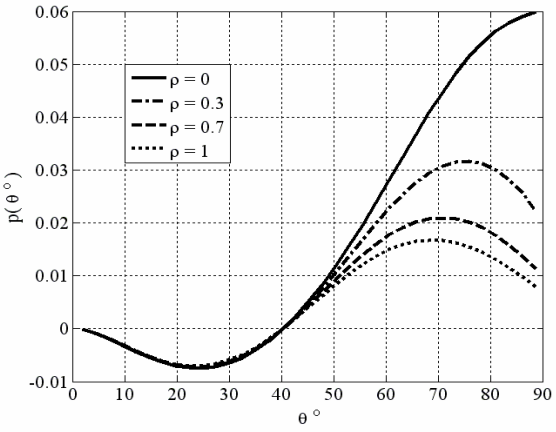

Figure 4. $p(\theta)$ within forward hemisphere for Mie-Haze L scattering with different reflectance coefficients of the bottom.

Let's consider the following parameters for this case: Λ = 0.9 and τ = 1. The results are shown on Figure 4 (forward hemisphere of bottom boundary – the radiation transmitted through the slab) and Figure 5 (backward hemisphere of the top boundary – the radiation reflected from the slab). The reflectance coefficients are ρ = 0 (solid line), ρ = 0.3 (dash-dot), ρ = 0.7 (dashed), ρ = 1 (dots). One can see that depolarization properties of the bottom reflectance influence greatly upon the polarization state of radiation – depolarization processing while bottom reflectance reinforce the depolarization process while multiple scattering inside the slab itself.

But if the bottom is embedded deep enough it will give notably weaker influence upon the polarization state of the reflected

radiation. Figure 6 give the result for the reflected polarization state of radiation for $\tau = 7$ optical thickness. The albedo and the irradiance angle are the same compared with the result given above, and the reflecting properties of the bottom boundary are described by the following coefficients: $\rho = 0$ (solid line), $\rho = 0.5$ (dash-dot), $\rho = 1$ (dashed).

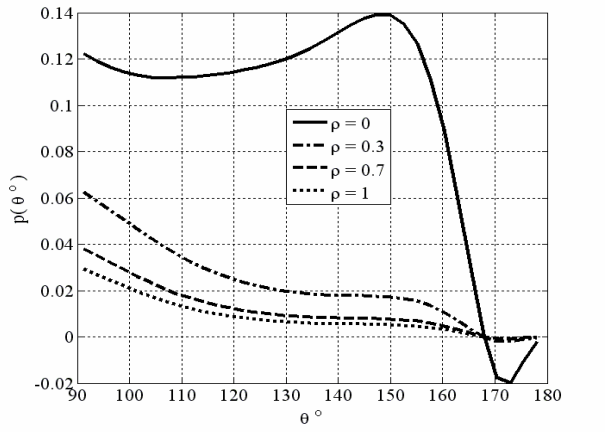

Figure 5. $p(\theta)$within backward hemisphere for Mie-Haze L scattering with different reflectance coefficients of the bottom.

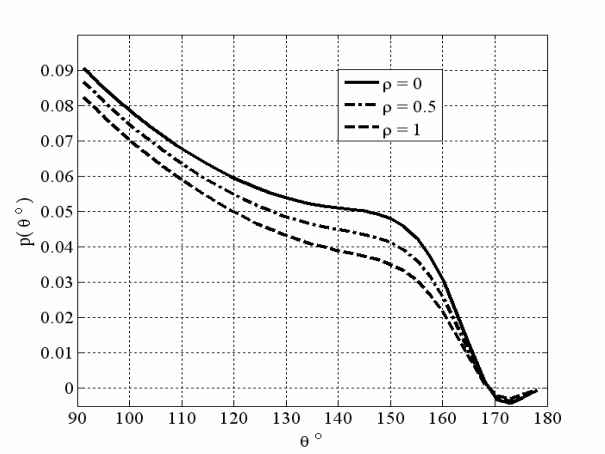

Figure 6. The same as on Figure 5 but for more embedded diffusely reflecting bottom.

Figure 7 demonstrates the influence of the reflecting bottom upon the Umov's law: the module of polarization state of light increasing together with the decreasing of single scattering albedo Λ. This is true for completely absorbing bottom – solid and dashed lines on the figure represents the PPC for $\Lambda = 0.9$ and $\Lambda=0.1$ respectively and for non-reflecting bottom. But for the case $\rho = 0.5$ this statement falls and a more complicated dependence takes place. The total optical thickness is $\tau = 1$ for the case and the PPC for transmitted radiation is shown on Figure 8.

4. POLAR-PHASE CURVES

The polar-phase curves (PPC) that we present in this chapter are the dependences of polarization state (4) with respect to the angle between the direction of slab's irradiance $\hat{\mathbf{l}}_0$ and the reflecting direction $\hat{\mathbf{l}}$ with the same zenith as $\hat{\mathbf{l}}_0$, i.e. $\hat{\mathbf{l}} \asymp \hat{\mathbf{l}}_R$ is the direction of "mirror" reflectance (but $\hat{\mathbf{l}}_R$ is really caused by multiple scattering). If we note $\phi = \mathrm{acos}(\hat{\mathbf{l}}_0 \hat{\mathbf{l}}_R)$ than PPC is the dependence $p(\cos\phi)$. Naturally $\phi \in [0..180]$, but it is well known that the slab is a good approximation for a planetary atmosphere not for arbitrary zenith angles of observation – no more than 75^o for zenith angle is recommended to assume (McCartney, 1977). That is why we'll give PPC with respect to $\phi \in [0..140]$ - restricted by double maximum zenith angle.

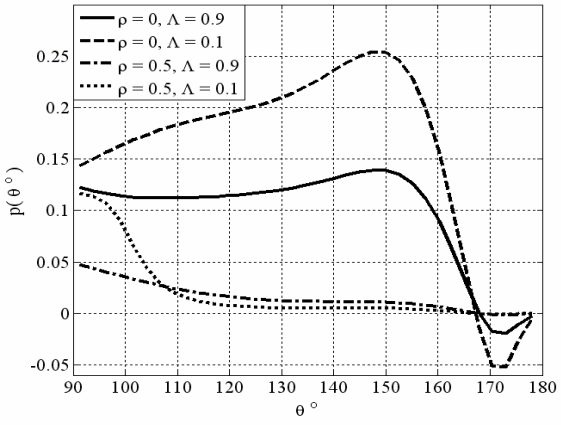

Figure 7. The polarization state $p(\theta)$ of reflected radiation for different Λ and ρ simultaneously.

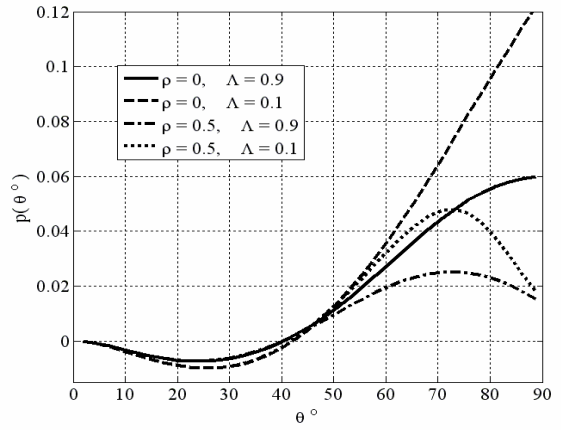

Figure 8. The same as on Figure 7 but for transmitted radiation.

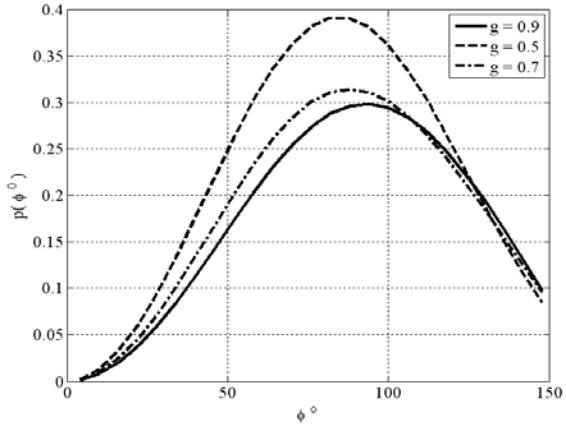

Figure 9. PPC for HG scattering with different anisotropy.

First of all we consider some PPCs for HG scattering with different scattering properties defined by average scattering cosine $g = 0.9$ (solid line), $g = 0.7$ (dash-dot), $g = 0.5$ (dashed) (Figure 9). The computation parameters, $P_m = 0.8$, $Q_m = 0$, $\Lambda = 0.8$, $\tau = 1$.

Next point – Rayleigh scattering for different optical thicknesses of the slab (Figure 10). We consider $\tau = 1$, $\Lambda = 0.9$ (solid line), $\Lambda = 0.5$ (dash-dot), $\Lambda = 0.1$ (dashed). Negative values for p are determined by reference plane selection. Umov's law is evident for this case.

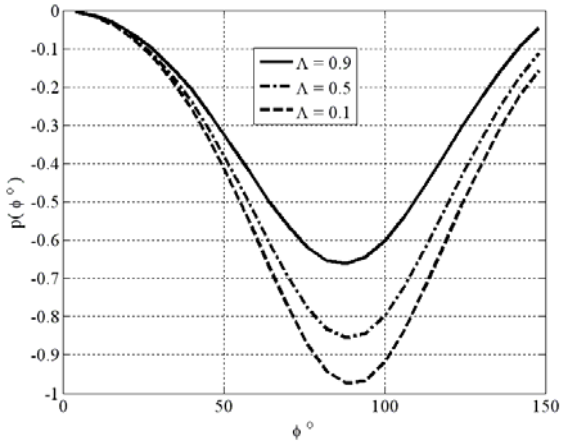

Figure 10. PPC for Rayleigh scattering and different albedo.

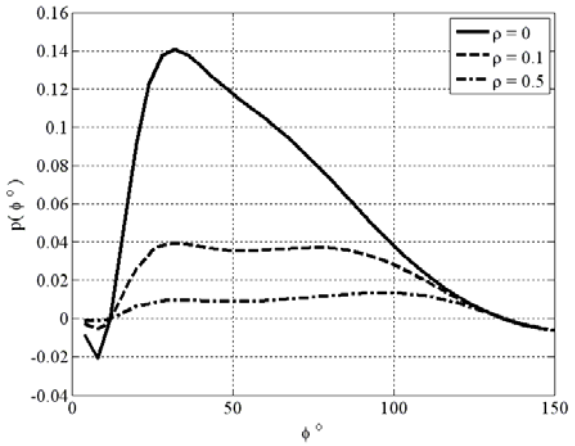

Figure 11. PPC for Water Haze L scattering and different bottom's reflecting properties.

And finally we show Mie (Haze L) scattering for different bottom's reflecting properties. We consider $\tau = 1$, $\Lambda = 0.9$ and $\rho = 0$ (solid line), $\rho = 0.1$ (dashed), $\Lambda = 0.5$ (dash-dot). Diffuse bottom reflection gives great influence upon PPC – depolarization is remarkable. Figure 11 shows the results.

5. CONCLUSION

We would like to conclude with the following: bottom reflectance influence greatly upon the PPC of the reflected light. That is why for the sake of completeness a mathematical model of polarized radiative transfer must include arbitrary Mueller matrix to describe the reflectance more precisely.

And the second point: the computational efficiency of the proposed method enfeebles for the simple slab geometry (one-dimensional problem) because of more complicated form for the source function compared with standard method. But for the case of 3D scattering no "forward" or "backward" scattering presents– the smoothness of the computed regular part is of a great importance. That is why we use the slab only to test the model and will direct our efforts on the solution of 3D polarized radiative transfer problems.

REFERENCES

Astakhov, I.E., Budak, V.P., Lisitsin, D.V., and Selivanov, V.A., 1994, Solution of the vector radiative transfer equation in the small-angle approximation of the spherical harmonics method, *Atmospheric and Oceanic Optics Journal*, **7**, 398 – 402.

Budak, V.P., Korkin, S.V., 2008a. On the solution of vectorial radiative transfer equation in arbitrary three-dimensional turbid medium with anisotropic scattering. *Journal of Quantitative Spectroscopy & Radiative Transfer*, **64**, 220 – 234.

Budak, V.P., Korkin, S.V., 2008b. The aerosol influence upon the polarization state of the atmosphere solar radiation. *International Journal of Remote Sensing* **(Currently in press)**

Budak, V.P., Kozelskii, A.V., Savitskii, E.N., 2004, Improvement of the spherical harmonics method convergence at strongly anisotropic scattering. *Atmospheric and Oceanic Optics Journal*, **17**, 28 – 33.

Chandrasekhar, S., 1960, *Radiative transfer* (New York: Dover).

Deirmendjian, D., 1969, *Electromagnetic scattering of spherical polydispersions* (New York: American Elsevier Publishing Company, Inc.).

Gelfand, I.M., Minlos, R.A., Shapiro, Z.Ya., 1963, *Representations of the rotation and Lorentz groups and their applications* (Oxford: Pergamon Press).

Hovenier, J.W., and van der Mee, C.V.M., 1996, Testing scattering matrices: a compendium of recipes. *Journal of Quantitative Spectroscopy & Radiative Transfer*, **55** (5), 649 – 661.

Karp, A.H., Greenstadt, J., Fillmore, J.A., 1980, Radiative transfer through an arbitrary thick scattering atmosphere. *Journal of Quantitative Spectroscopy & Radiative Transfer*, **24** (5), 39 – 406.

Kuščer, I., Ribarič, M., 1959, Matrix Formalism in the Theory of Diffusion of Light. *Optica Acta*, **6**, 42 – 51.

McCartney, E.J., 1977, Optics of the Atmosphere. Scattering by Molecules and Particles (New York: John Wiley and Sons).

Siewert, C.E., 2000, A discrete-ordinates solution for radiative-transfer models that include polarization effects. *Journal of Quantitative Spectroscopy & Radiative Transfer*, **64**, 227 – 254.

ACKNOWLEDGMENTS

The author appreciate the members of "The Light Field in the Turbid Medium" scientific seminar held in the Light Engineering Department in Moscow Power-Engineering Institute (TU).